

Is a Stronger Building also Greener? Influence of Seismic Design Decisions on Building Life-Cycle Economic and Environmental Impacts

S.J. Welsh-Huggins & A.B. Liel

University of Colorado Boulder, Boulder, Colorado, USA

ABSTRACT: This study investigates the idea that “green” buildings should be designed for higher earthquake and other extreme loads to reduce the environmental impacts of post-hazard repairs. To do so, we consider the seismic performance and environmental impact of reinforced concrete frame buildings with varying strengths, by quantifying CO₂ equivalent emissions, or embodied carbon, in the context of seismic design decisions. The results suggest that larger structural members of stronger buildings (above-code designs) lead to higher upfront embodied carbon, whereas manufacturing of smaller structural members for weaker buildings produces less upfront embodied carbon. In terms of post-earthquake impacts, we quantify the expected annual embodied carbon from repair activities (considering contributions from a range of possible future seismic hazard events). The results demonstrate that stronger, above-code buildings have lower expected repair costs and embodied carbon than weaker code-compliant or below-code variations, suggesting that—with respect to annualized impacts—stronger buildings are in fact “greener.” Deaggregating these results reveals that at lower hazard levels (representing more frequent events), stronger buildings experience lower drift and acceleration demands than code-compliant or below-code variants, leading to lower seismic losses and embodied carbon. However, at higher hazard levels, increased stiffness from lower fundamental periods of stronger buildings can increase the influence of nonstructural losses on repair embodied carbon generating somewhat higher emissions. Although certain details differed, the overall trends were consistent between space and perimeter frames.

1 INTRODUCTION

Two distinct, but related, trends characterize the 21st century building stock. On one hand, the number of buildings with green or sustainable features is growing rapidly. At the same time, there is increasing exposure to extreme hazard events due to larger populations, dense urban environments, and a changing climate. A number of recent documents have proposed that designing buildings to higher loads for seismic and other extreme load cases may reduce environmental impacts from post-hazard repairs (e.g. PCA 2012; Chiu et al. 2013). This idea demonstrates a broader paradigm shift recognizing that building for resilience is building sustainably. Recent studies have explored the relationship between seismic design, damage, and post-hazard environmental impact (Arroyo et al. 2014; Bocchini et al. 2014; Hossain and Gencturk 2014). In addition, other studies have examined the impacts of design strength on seismic-induced economic losses (e.g.,

Haselton et al. 2011; Ramirez et al. 2012). However, researchers have yet to explicitly and systematically quantify environmental tradeoffs associated with enhanced seismic design. Our study seeks to fill this gap by evaluating the influence of seismic design strength on environmental impact (quantified here as embodied carbon) for a set of reinforced concrete (RC) buildings with varying levels of design strength.

2 BACKGROUND

The joint evaluation of building hazard resistance and life-cycle environmental impact is a still-growing field of research and practice. Previous studies have quantified CO₂ emissions and economic losses from building construction and post-earthquake repairs for specific cases. For example, Hossain and Gencturk (2014) compared life-cycle environmental impacts of seismic losses for two RC buildings, one with a low initial cost and high interstory drift ratios during dynamic analysis and the other with a higher upfront cost and low interstory drift. The study conducted

Pareto optimization to minimize member size and reinforcement ratios, given the desired cost and drift constraints. They found that larger seismic losses from the less-expensive building incurred much higher environmental impacts from post-hazard repairs than the more expensive building. However, the study also suggested that the overall life-cycle environmental impact of the low-cost building was 40% lower than that of the high-cost building because of lower material volumes used in construction and removed during end-of-life disposal. In a related study, Gencturk et al. (2016) demonstrated that investing more money upfront in larger member sizes could reduce seismic losses, but increased initial environmental impact due to greater material consumption during construction. The opposite was true if smaller member sizes or less steel was used.

Welsh-Huggins and Liel (2016) indirectly considered the influence of member size and design strength on environmental and seismic performance in an assessment of “up-sizing” members to support dead and live loads for vegetated roof systems. That study found that larger beam and columns for the green roof buildings increased initial embodied CO₂. The study also showed that the buildings with larger roof loads (and hence higher member sizes) experienced more seismic damage from rare, high consequence earthquakes, but better withstood ground shaking of more frequent, lower consequence events. Greater repair demands also increased repair CO₂ emissions, due in part to the difference in material volumes for restoration of the larger structural members.

3 ASSESSMENT OF CASE STUDY BUILDINGS

3.1 Case study building designs

The study here of the influence of building strength on life-cycle impacts investigates eight commercial buildings designed for Los Angeles. The basic design of these modern four-story office buildings is adopted from Goulet et al. (2007) and Haselton et al. (2011), for an archetypical office building. Each building has a floor area of 120 ft. by 180 ft. with six RC frame lines resisting lateral loads in each direction. The story height at the first story is 15 ft.; all others are 13 ft; column spacing is 30 ft. The case study site in Los Angeles places the building in seismic design category D (ASCE 2010). This site has a design spectral acceleration for short periods (S_{DS}) of 1.0g and at 1s (S_{D1}) of 0.6g.

Our study considers varying configurations of special moment RC perimeter and space frames, where each building is designed to be code-conforming in all respects, except design strength.

For each building, we vary the so-called R factor, which is a direct modifier on structural strength in the design process. The International Building Code (ICC 2009) specifies a value of $R = 8$ for special RC moment frames. Our study considers this code-specified value, as well as stronger ($R < 8$) and weaker ($R > 8$) variations. Designing for lower R factors requires larger member sizes and greater areas of reinforcing steel to satisfy the increased strength requirements. The larger member sizes also make the stronger buildings stiffer than the code-compliant and below-code designs, producing smaller fundamental periods for the above-code buildings (and vice versa for the weaker buildings).

Tables 1 and Table 2 present the structural member dimensions for the perimeter and space frames, respectively. The space frames have the same member dimensions for interior and exterior frame lines. The perimeter frames employ smaller (12.5 in x 12.5 in) gravity columns on the interior frame lines.

Table 1. Perimeter frame design: base shear, member dimensions, and fundamental periods.

R Value	Design Base Shear ¹ (kips)	Column Size (b x h; in x in)	Beam Size (b x h; in x in)	Period ² (T ₁), sec.
4	1,264	44x50	44x52	0.53
8	580	34x30 (corners), 38x30 (center columns)	34x30	1.15
12	386	30x30 (corners), 36x30 (center columns)	30x34	1.16

Table 2. Space frame design: base shear, member dimensions, and fundamental periods.

R Value	Design Base Shear ¹ (kips)	Column Size (b x h; in x in)	Beam Size (b x h; in x in)	Period ² (T ₁), sec.
4	386	30x30	30x36 (floors 1-2), 30x30 (floors 3-4)	0.74
5.3	290	30x30	30x34 (floors 1-2), 30x28 (floors 3-4)	0.78
8	193	30x30	30x30 (floors 1-2), 30x24 (floors 3-4)	0.86
10	156	28x28	28x28	0.92
12	129	28x28	28x28 (floors 1-2), 28x26 (floors 3-4)	0.97

¹Design base shear: per frame in units of kips

²Period from eigenvalue analysis of simulation models (section 3), considering cracked section properties.

3.2 Nonlinear structural modeling

The *OpenSEES* seismic analysis program (PEER 2014) is used to conduct nonlinear analysis of two-dimensional, three-bay models of the buildings considered here. Beam-columns are modeled with elastic elements and concentrated hinge springs, i.e. a lumped plasticity approach. These hinges are assigned a material model developed by Ibarra et al. (2005), which is capable of capturing the effect of strain softening at large deformations associated with concrete spalling and rebar buckling. The hinge model can also capture cyclic deterioration and accounts for bond-slip. The properties of the hinge are calibrated to experimental results of more than 250 concrete columns, such that modeling of different components represents differences in design and detailing. For dynamic analysis, the buildings are assumed to have 5% Rayleigh damping applied to the first and third modes, and assigned only to the models' elastic elements. More details about the structural modeling approach are available in (Haselton et al. 2011; Haselton and Deierlein 2007).

Figure 1 shows the results of static pushover analysis for the space frames, demonstrating that decreased R factors increases design base shear and the subsequent lateral strength capacity for a given structure.

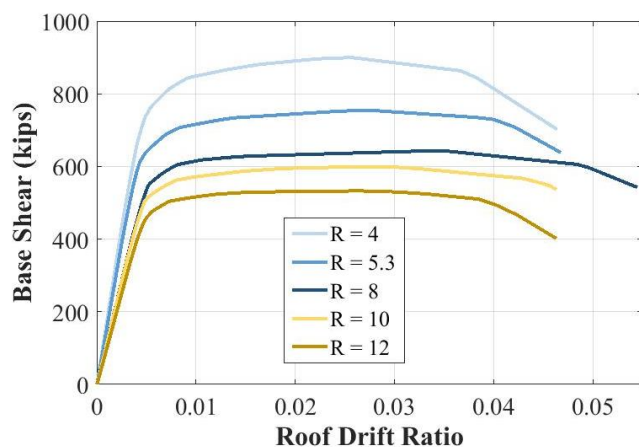


Figure 1. Results of static pushover analysis for space frame buildings, showing higher peak strengths for buildings designed for lower R factors.

Larger member sizes for the above-code (lower R) buildings subsequently necessitate larger volumes of structural steel and concrete for initial construction.

Figure 2 shows the total embodied carbon associated with upfront production and manufacturing of all structural and nonstructural components, compared to the lateral strength of each building (presented in terms of maximum base shear from pushover analysis). Embodied carbon is the total amount of greenhouse gas emissions, converted to CO₂ equivalents, required to produce a given material or building product. CO₂ equivalents compare emissions from different greenhouse gases with respect to their contribution to climate change. The

manufacturing of concrete and steel are carbon-intensive activities that dominate the total embodied carbon of a building. Therefore, material manufacturing for construction of the above-code buildings here leads to higher upfront embodied carbon than for the code-minimum or below-code design variants (currently this study does not include sources of uncertainty in quantification of embodied carbon). The embodied carbon from manufacturing materials for construction of the code-compliant (R = 8) space frame is equivalent to the greenhouse gas emissions from driving a passenger vehicle almost 1,800,000 miles (EPA 2016).

There is not, however, a linear relationship between design base shear, material volumes, and embodied carbon. In the case of the space frame variations, the above-code building produces only a marginally greater volume of embodied carbon than the weaker structures. The weaker building designs are dominated by building code considerations separate from design base shear, such as drift limits and gravity loads. In the case of the gravity-load-dominated space frames, these buildings do not require drastic differences in beam and column dimensions to achieve design strengths. Member sizes of perimeter frames, which have lateral load dominated designs, are more sensitive to changes in design strength requirements.

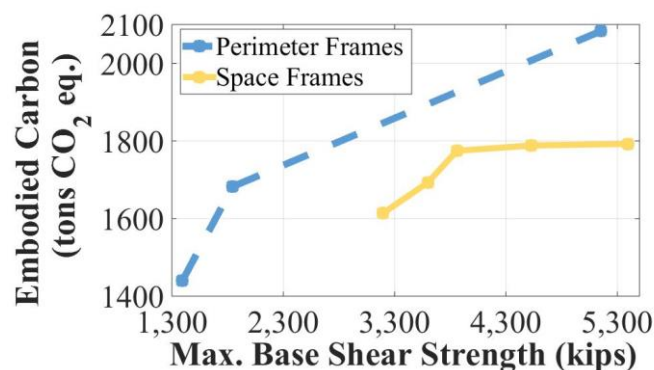


Figure 2. Total embodied carbon (tons CO₂ equivalents) from material manufacturing for construction of space and perimeter frames, compared to maximum base shear strength.

3.3 Structural response under earthquake shaking

We compute the seismic performance of the models using a procedure called Incremental Dynamic Analysis (IDA). In IDA, acceleration time histories are scaled first to a value for $S_a(T_1)$. For each scaled ground motion in an IDA, the building's structural response is analyzed (Vamvatsikos and Cornell 2002). The scale factor for each record is increased until the structure collapses. Here, we identify collapse as occurring when interstory drifts greater than 12% are recorded in any story, following Haselton et al. (2011). We employ a suite of thirty strong ground motions from Vamvatsikos and Cornell (2006) recorded during California earthquakes with magnitudes between 6.5-6.9, at firm

sites with site-to-source distances ranging from 15-33 km. These ground motions records are considered representative of the type of crustal ground motions expected at our site. We assess the seismic performance of our models under nine different hazard levels, ranging in probability of exceedance from 50% in 50 years (referred to here as Hazard Level 1, or HL1) to 1% in 50 years (HL9).

Figure 3 presents the collapse fragility curves obtained for the space frame buildings. The IDA results (quantified in terms of $Sa(T = 1.00s)$ for all cases) show that the stronger buildings ($R < 8$) have higher collapse capacities than the weaker code-minimum and non-code compliant frames. Although the stronger models exhibit higher collapse capacities, their increased stiffness and smaller fundamental periods causes them to dynamically experience larger floor accelerations, and smaller interstory drifts than for the below-code variants at lower hazard levels. At higher hazard levels the more inelastic response of the weaker buildings takes over, making this trend more complex.

The perimeter frames demonstrate similar trends in the results of their IDA with design R factor, but produce systematically lower collapse capacities than their space frames counterparts. In addition, the small period of the strongest perimeter frame significantly increases the spectral acceleration experienced, such that the seismic demand placed on this model is greater than that of its space frame equivalent.

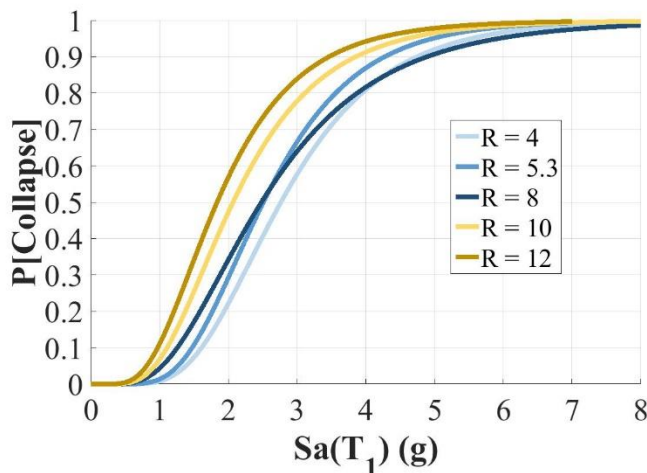


Figure 3. Collapse fragility curves for space frame buildings.

3.4 Seismic loss analysis

Loss estimation refers to probabilistic analysis of building performance under seismic loading in terms of damage and repair costs. The basis for our loss analysis comes from seismic performance and probabilistic loss-estimation procedures developed by the FEMA P-58 project (ATC 2012). The Seismic Performance Prediction Program (SP3), developed by the Haselton Baker Risk Group, is a web-based tool implementing the FEMA-58 loss estimation calculations (SP3 2016). Damage is quantified using

fragility curves that express the probability that each component (structural or nonstructural) is in or exceeds a specified damage state (DS) as a function of the seismic demands on a building. Each damage state is linked to the cost of repairing a normative unit of the given building component as a result of the incurred damage condition.

For each hazard level, the total repair cost is computed as a sum of the expected annual repair cost at that shaking level for no collapse (defined further in Section **Error! Reference source not found.**), and the cost of total building replacement in the case of collapse. The probability of collapse at each hazard level is interrogated from the collapse fragilities developed from the IDA results. If collapse occurs, we assume that the entire building must be replaced, with a cost of \$230/square foot times the gross building area for the space frames (SP3 2016). The perimeter frames have a slightly lower replacement cost (\$220/square foot). These costs are reasonable approximations for the purposes of this study, although they do not account for economies of scale in construction pricing for the large member sizes of the stronger buildings.

Figure 4 shows the median total building repair costs for the space frames, based on the SP3 loss analysis outcomes, as a function of hazard (ground shaking intensity) level. At the lowest shaking intensities, all buildings incur similar total repair costs, with marginal differences between the strongest and weakest buildings. At the highest levels of shaking, however, stronger buildings exhibit significantly improved performance and thus decreased seismic losses due to their higher collapse capacities. The greater probability of collapse for the weaker buildings at higher hazard levels results in higher potential repair costs for these buildings.

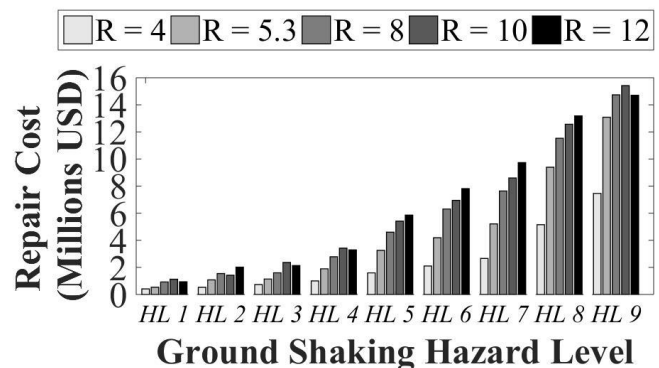


Figure 4. Total building repair costs at nine levels of ground shaking for space frame buildings (results computed at $Sa(T_1)$ for each building and presented at each of nine hazard levels).

The perimeter frames show the same trends in losses, although repair costs are similar for the code-compliant and below-code frames, due to similar collapse capacities. The greatly increased strength (and associated stiffness) of the above-code perimeter

frame results in correspondingly much lower seismic losses at each hazard level.

3.5 Environmental impact analysis

Process-based life-cycle inventory analysis computes the main input and output flows of energy and materials (e.g., emissions) of a functional unit of analysis (EPA 2008). This study considers each building as a functional unit. We utilize life-cycle inventory (LCI) data to estimate energy/material flows, and associated emissions (Cook 2014) generated by the manufacturing of materials for pre-service life construction and building repairs of post-earthquake damage.

We use the process-based life-cycle software SimaPro to organize environmental impact calculations for all building materials in terms of both initial manufacturing for construction and for materials needed in post-earthquake repairs. SimaPro organizes life-cycle inventory quantities from the Ecoinvent database. Ecoinvent is a well-established and comprehensive source, containing over 10,000 different processes (Goedkoop et al. 2013). In SimaPro, the impact of inventory processes are allocated using the EPA's Tool for the Reduction and Assessment of Chemical and other Environmental Impacts (TRACI). While LCI presents raw emissions from each process, the TRACI methodology quantifies how these emissions combine together to produce environmental impacts, including associated chemical releases (EPA 2008).

To quantify environmental impacts, we consider only embodied carbon associated with material manufacturing. On-site construction, transportation of materials, and demolition and debris removal are outside the scope of calculations for both upfront and post-earthquake embodied carbon impacts.

Welsh-Huggins and Liel (2016) details our approach to translating the damaged components and associated building repair costs computed in seismic loss analysis into material volumes for specific repair actions. Specifically, we convert Monte Carlo analysis results for probabilistic losses of each component into volumes of materials needed to repair these damaged units, considering 10,000 realizations at each hazard level. After computing these material repair volumes for each realization, we multiply the respective material quantities by the unit embodied carbon. The final output for each building is a lognormal distribution of the embodied carbon associated with repair activities at each hazard level, which accounts for uncertainties in the damage and losses at each hazard level. For realizations that experience collapse, we assume that the entire building must be replaced. Therefore, replacement embodied carbon for each building is equal to its respective upfront embodied carbon, *i.e.* the carbon

emissions generated by re-manufacturing all structural and nonstructural components to restore the building to full functionality for the remainder of its service life.

Figure 5 presents the median total embodied carbon from post-hazard repairs at each hazard level. At ground shaking intensities with probabilities of exceedance greater than or equal to 5% in 50 years (*i.e.*, HL1-7), the embodied carbon impact for the space and perimeter design variants exhibit a similar trend. At these shaking intensities weaker buildings experience greater damage than the stronger buildings. Greater damage to weaker structures requires larger volumes of materials for repairs, producing higher CO₂ emissions from manufacturing materials for post-earthquake repairs.

The findings from this study, however, highlight the influence of fundamental period on structural response and associated damage to nonstructural components. Stiffer buildings, with lower fundamental periods, experience lower interstory drifts and higher peak floor accelerations. These buildings typically have higher nonstructural losses, because fragilities of most nonstructural components are correlated to peak floor accelerations. When probabilities of collapse of two buildings are similar, the building with higher nonstructural losses will likely also produce higher total embodied carbon than the building with a slightly greater probability of collapse. This trend is due to the amount of embodied carbon associated with nonstructural repairs. For example, for suspended ceiling tiles that enter their DS2, the FEMA P-58 methodology recommends replacing 20% of each damaged normative ceiling tile unit (2,500 ft²) on a floor (ATC 2012). Replacement of these damaged tiles requires 39 ft³ of glass fiber tiles and 1.9 ft³ of steel tracking per normative unit, producing almost four tons of embodied carbon. In contrast, non-collapse damage (at the shaking intensities experienced in this analysis) to structural components tends to involve concrete patching and other actions that generate lower CO₂ emissions.

The difference in repair carbon emissions for the code-compliant and below-code space frames at the two highest hazard levels demonstrate the varying influence of collapse capacity and nonstructural losses on post-earthquake embodied carbon. The code-compliant space frame has only a slightly higher collapse capacity (lower collapse probability at these upper hazard levels) than the below-code frames, but nonlinearities in structural response and the increased stiffness of this building causes it experience higher peak floor accelerations than the weaker frames. Therefore, at HL8 and HL9, the code-compliant space frame actually generates more embodied carbon than below-code designs, due to greater contribution from acceleration-sensitive nonstructural components.

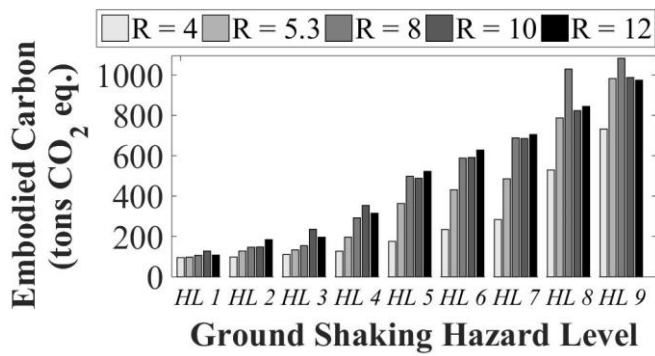


Figure 5. Total embodied carbon (tons CO₂ equivalent) from repair activities at nine hazard levels for the space frames.

3.6 Life-cycle tradeoffs

This study considers how variations in strength (correlated to design base shear) and differing framing techniques (space vs. perimeter) affect life-cycle embodied carbon. The findings support a holistic building life-cycle assessment with respect to both economic and environmental impacts. However, one challenge in presentation of results is the differing metrics of economic value (dollars) and environmental impact (embodied carbon in terms of CO₂ equivalents). The complexity of real-world decision-making encourages assessment of results using their respective metrics, because converting results to the units (*e.g.*, CO₂ equivalents to dollars) limits our ability to analyze different temporal and spatial considerations of problems with equally-weighted economic and environmental pillars (Kajikawa 2008; Schweikert et al. 2015).

One approach to present multi-criteria results is quantification of the expected annualized losses (EAL) for each building. We compute both the expected annual repair cost (dollar losses) and expected annual embodied carbon (emissions-related losses) from post-earthquake repairs. Expected annualized losses are based on the probability of exceedance of each hazard level and the dollar or CO₂ emission consequences of shaking intensities at each respective hazard level (Baker and Cornell 2003).

Figure 6 presents the EALs for each space frame, normalized by each building's total replacement cost (in terms of either dollars or embodied carbon). The EALs are presented here as annuities, not discounted to present value, due to the challenge of selecting appropriate discount rates for environmental impacts like embodied carbon (Kajikawa 2008). The results show that increasing lateral strength decreases both annual economic loss and annual embodied carbon impact from post-earthquake repairs. The code-compliant and below-code perimeter frames have higher annual economic losses than their space frame counterparts, because of increased collapse probabilities, but slightly lower expected annual embodied carbon, due to lower CO₂ emissions for total replacement of their smaller structural members.

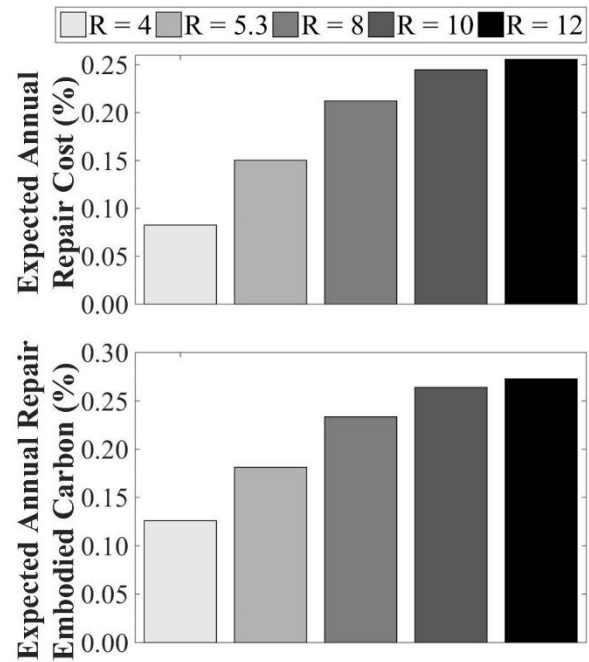


Figure 6. Expected annualized losses for space frame designs (expressed as percentages of total replacement cost and total replacement embodied carbon).

Next we analyze the influence of the percentages of nonstructural and structural repair impacts on total seismic losses at each hazard level, in terms of economic cost and embodied carbon. For this purpose we deaggregate losses by the contributing component or “performance group.” We define the cost of total building replacement (in the event of collapse) as a separate “performance group” to evaluate the impact of rebuilding the entire structure against that of only repairing other components.

The structural and nonstructural components that contribute to the seismic loss at each hazard level depends on the metric of analysis, either economic loss or embodied carbon, and the associated repair cost or CO₂ emission consequences per damaged unit. As discussed in Section 3.5, depending on the damage state of repair materials, certain nonstructural performance groups (such as ceiling tiles, interior partitions, or water conveyance pipes) may require more CO₂-intensive repairs than other components with higher economic costs (like beam-columns or concrete cladding). For all of the study buildings, the high cost consequence for repairs to exterior concrete cladding leads this component's losses to contribute almost 50% of total repair economic costs of each hazard level. The sub-set of components that contribute the remainder of seismic loss outcomes at each hazard level depends on the specific seismic demand experienced by each building and its resulting structural and nonstructural response.

Figure 7 presents the deaggregated component contribution to repair dollars and repair embodied carbon for the code-compliant space frame (R = 8). For this building, the non-concrete cladding economic losses at low levels of shaking are

dominated by repairs to the interior partitions and ceiling tiles. As ground shaking increases, probability of collapse increases and structural (beam-column) components are more likely to experience higher damage states, thus increasing the contribution of these two performance groups to hazard level economic and environmental loss.

Although economic costs to repair exterior concrete cladding that enter their respective first damage state are greater than those to repair other nonstructural components in their DS1 conditions—due to differences in manufacturing and installation economies of scale—the embodied carbon produced from concrete cladding repairs is low. By comparison, the embodied carbon to repair ceiling tiles and interior partitions at a given hazard level outweighs that of almost all other performance groups at the same shaking intensity. It is only when beam-columns enter higher damage states and require more carbon-intensive repairs and when the probability of collapse (and thus probability of total building replacement) increases, that the relative contribution of embodied carbon from partition and ceiling tile repairs diminishes slightly.

This finding presents important tradeoffs for designers to consider with respect to the prioritization of different metrics and their associated influences on the life-cycle costs of a potential new structure.

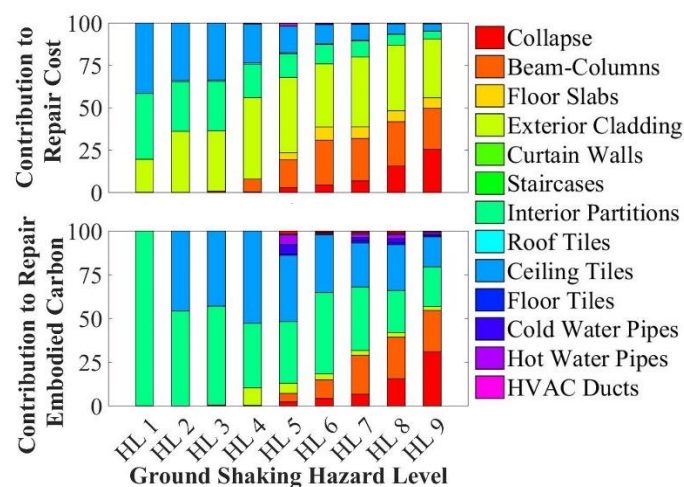


Figure 7. Performance group contribution to repair cost and repair embodied carbon for code-compliant space frame ($R = 8$). (Results are presented as annuities, without discounting to present value. Sprinkler and sanitary waste pipe contributions are negligible in both categories, so are not shown here).

4 CONCLUSIONS

This study responds to previously untested recommendations that designing a structure for higher seismic (and/or other forces) is a green design strategy. The study objective is to investigate whether designing for higher levels of strength can in fact yield a “greener” building, measured here in terms of life-cycle embodied carbon.

The results demonstrate that increasing lateral strength (equivalent to decreasing the response modification coefficient, or R factor) requires larger member sizes to satisfy increases in design base shear. The larger structural members are associated with increased upfront embodied carbon, due to the carbon-intensive processes of manufacturing structural concrete and reinforcing steel. On the other hand, increasing lateral strength decreases repair costs (economic losses) at all ground shaking hazard levels assessed here. When quantifying the contribution to repair embodied carbon over multiple hazard levels, increasing lateral strength also decreases expected annual carbon emissions. Therefore, increasing lateral design strength can produce “greener” buildings, in terms of expected annual embodied carbon, considering multiple possible contributions to the seismic hazard at the site of interest from the occurrence of at most one earthquake during the building’s lifespan.

We have shown here, however, that the trends relating strength and sustainability to seismic performance are highly complex. Above-code lateral strength also improves the life-cycle sustainability of buildings that experience ground shaking events with probabilities of exceedance greater than 2% in 50 years. However, the relationship between lateral strength and seismic repair embodied carbon depends on the fundamental period and associated stiffness of each structure. Our results show that when structures have similar probabilities of collapse at high-intensity, low probability ground shaking events, stronger designs—which tend to also have lower fundamental periods—can incur greater embodied carbon from repairs activities than do weaker designs. These higher carbon emissions arise when nonstructural components incur greater damage as a result of larger peak floor accelerations felt by stiffer (albeit stronger) frames. In addition, the results show that at certain levels of shaking intensity, the associated repair activities for nonstructural groups (like ceiling tiles or interior partitions) are more carbon intensive than repairs for structural components that experience similar seismic demand.

Our findings suggest that decision-makers will need to weigh concerns for future earthquake events and their associated potential economic and environmental losses with the upfront environmental impact of constructing stronger buildings. For example, lower repair carbon emissions at moderately-probable ground shaking events for stronger buildings must be balanced against high upfront embodied carbon from manufacturing larger structural members. These buildings may also have potentially higher CO_2 emissions than weaker designs at high levels of ground shaking intensity, due to increased stiffness. Once goals for collapse capacity and life-safety have been met, building owners and design teams could consider prioritizing design

objectives by designing a building with the objective of not exceeding a specified threshold life-cycle embodied carbon. Additionally, member size is not the only indicator of building strength. Structural engineers and building owners should strive to design more hazard-resistant buildings, without necessarily “up-sizing” structural members to meet these goals.

Future work could also investigate different structural systems from the ones considered in this study, to better quantify the sensitivity of repair CO₂ emissions to nonstructural losses for different building systems. Additional studies also should consider how to quantify embodied carbon in terms of present value, while still accounting for ethical issues related to the intergenerational equity of future environmental impacts.

5 ACKNOWLEDGMENTS

This research is made possible through the support of the National Science Foundation, Award Number #1234503. Any opinions, findings, and conclusions or recommendations expressed in this material are those of the authors and do not necessarily reflect the views of the National Science Foundation. The authors gratefully acknowledge the Haselton Baker Risk Group for providing access to their SP3 software.

6 REFERENCES

- American Society of Civil Engineers (ASCE). (2010). *Minimum design loads for buildings and other structures: ASCE/SEI 7-10*. Reston, VA: ASCE.
- Applied Technology Council (ATC). (2012). Seismic performance of assessment of buildings. Applied Technology Council and Federal Emergency Management Agency (FEMA P-58), 1&2, Sept. 2012.
- Arroyo, D., Ordaz, M., and Teran-Gilmore, A. (2015). Seismic loss estimation and environmental issues. *Earthquake Spectra*, 31, 1285-1308.
- Baker, J.W. and Cornell, C.A. (2003). Uncertainty specification and propagation for loss estimation using FOSM methods, PEER Technical Report 2003/07. Berkeley, California.
- Bocchini, P., Frangopol, D., Ummenhofer, T., and Zinke, T. (2014). Resilience and sustainability of civil infrastructure: toward a unified approach. *J. Infrastruct. Syst.*, 20, 04014004.
- Chiu, C. K., Chen, M. R., and Chiu, C. H. (2013). Financial and environmental payback periods of seismic retrofit investments for reinforced concrete buildings estimated using a novel method. *J. Archit. Eng.*, 19, 112–118.
- Cook, Sherri (2014). Sustainable wastewater management: modeling and decision strategies for unused medications and wastewater solids. (PhD thesis). Ann Arbor, MI: University of Michigan.
- Environmental Protection Agency (EPA) (2016). Greenhouse gas equivalencies calculator. (<http://www.epa.gov/energy/greenhouse-gas-equivalencies-calculator>).
- Environmental Protection Agency. (2008). Life cycle assessment: principles and practice. Cincinnati, OH: Scientific Applications International Corporation.
- Gencturk, B., Hossain, K., and Lahourpour, S. (2016). Life cycle sustainability assessment of RC buildings in seismic regions. *Eng. Struct.*, 110, 347–362.
- Goedkoop, M., Michiel, O., Leijting, J., Ponsioen, T., and Meijer, E. (2013). Introduction to LCA with SimaPro. Amersfoort, The Netherlands: PréSustainability.
- Goulet, C., Haselton, C. B., Mitrani-Reiser, J., Beck, J. L., Deierlein, G., Porter, K. A., & Stewart, J. P. (2007). Evaluation of the seismic performance of a code-conforming reinforced-concrete frame building—From seismic hazard to collapse safety and economic losses. *Earthquake Engng. Struct. Dyn.*, 36, 1973–1997.
- Haselton, C. B., Liel, A. B., Deierlein, G. G., Dean, B. S., & Chou, J. H. (2011). Seismic collapse safety of reinforced concrete buildings. I: assessment of ductile moment frames. *Journal of Structural Engineering*, 137, 481–491.
- Haselton, C. B., & Deierlein, G. G. (2007). Assessing seismic collapse safety of modern reinforced concrete moment frame buildings (TR No. 156). CA: John A. Blume Earthquake Engineering Center, Stanford University. John A. Blume Earthquake Engineering Center, Stanford University.
- Hossain, K. A., and Gencturk, B. (2014). Life-cycle environmental impact assessment of reinforced concrete buildings subjected to natural hazards. *J. Archit. Eng.*, doi: [http://dx.doi.org/10.1061/\(ASCE\)AE.1943-5568.0000153](http://dx.doi.org/10.1061/(ASCE)AE.1943-5568.0000153), A4014001, in press.
- Ibarra, L. F., et al. (2005). Hysteretic models that incorporate strength and stiffness deterioration. *Earthquake Engng. Struct. Dyn.*, 34, 1489–1511.
- International Code Council. (2009). 2009 international building code. ICC: Country Club Hills, IL.
- Kajikawa, Y. (2008) Research core and framework of sustainability science. *Sustainability Science*, 3, 215–239.
- Pacific Earthquake Engineering Research Center (PEER). (2014). The open system for earthquake engineering simulation. (www.openssees.berkeley.org).
- Portland Cement Association (PCA). (2012). Functional resilience: prerequisite for green buildings. *Concrete Joint Sustainability Initiative*. (www.sustainableconcrete.org).
- Ramirez, C. M., Liel, A. B., Mitrani-Reiser, J., Haselton, C. B., Spear, A. D., Steiner, J., Miranda, E. (2012). Expected earthquake damage and repair costs in reinforced concrete frame buildings. *Earthquake Engng. Struct. Dyn.*, 41, 1455–1475.
- Schweikert, A., Chinowsky, P., Espinet, X. (2015). The triple bottom line: bringing a sustainability framework to prioritize climate change investments for infrastructure planning. *Proceedings of 95th Transportation Research Board Annual Meeting Proceedings*, Washington, D.C.
- Seismic Performance Prediction Program (SP3) (2016). “SP3.” Haselton Baker Risk Group. (<http://www.hbrisk.com/>).
- Welsh-Huggins, S. J. & Liel, A.B. (2016). A life-cycle framework for integrating green Building and hazard-resistant design: examining the seismic impacts of buildings with green roofs. *Structure and Infrastructure Engineering*, in press.
- Vamvatsikos, D., & Cornell, C. A. (2002). Incremental dynamic analysis. *Earthquake Engng. Struct. Dyn.*, 31, 491–514.
- Vamvatsikos, D., and Cornell, C.A. (2006). Direct estimation of the seismic demand and capacity of oscillators with multi-linear static pushovers through IDA. *Earthquake Engng. Struct. Dyn.*, 35, 1097–1117.